Journal of Alloys and Compounds 509 (2011) 6965–6968

Contents lists available at ScienceDirect

Journal of Alloys and Compounds

journal homepage: www.elsevier.com/locate/jallcom

Improved capacity and rate capability of Ru-doped and carbon-coated $Li_4Ti_5O_{12}$ anode material

Chih-Yuan Lin, Yi-Ruei Jhan, Jenq-Gong Duh*

Department of Materials Science and Engineering, NationalTsing-HuaUniversity, Hsinchu, Taiwan

ARTICLE INFO

Article history:
Received 7 January 2011
Received in revised form 28 March 2011
Accepted 2 April 2011
Available online 8 April 2011

Keywords:
Anode material
$Li_4Ti_5O_{12}$
$Li_4Ti_5O_{12}$/C
Ru-doped $Li_4Ti_5O_{12}$

ABSTRACT

Pure $Li_4Ti_5O_{12}$, modified $Li_4Ti_5O_{12}$/C, $Li_4Ru_{0.01}Ti_{4.99}O_{12}$ and $Li_4Ru_{0.01}Ti_{4.99}O_{12}$/C were successfully prepared by a modified solid-state method and its electrochemical properties were investigated. From the XRD patterns, the added sugar or doped Ru did not affect the spinel structure. The results of electrochemical properties revealed that $Li_4Ru_{0.01}Ti_{4.99}O_{12}$/C showed 120 and 110 mAh/g at 5 and 10 C rate after 100 charge/discharge cycles. $Li_4Ru_{0.01}Ti_{4.99}O_{12}$/C exhibited the best rate capability and the highest capacity at 5 and 10 C charge/discharge rate owing to the increase of electronic conductivity and the reduction of interface resistance between particles of $Li_4Ti_5O_{12}$.It is expected that the $Li_4Ru_{0.01}Ti_{4.99}O_{12}$/C will be a promising anode material to be used in high-rate lithium ion battery.

1. Introduction

Lithium-ion batteries are popular worldwide as power sources for wireless telephones, laptop computers and other electronic devices. Recently, applications of lithium ion batteries have diversified from high energy density to high power density and long life owing to environmental issues [1]. Generally, anode materials with a three-dimensional framework are more safe than two-dimensional compounds such as carbonous. One of the key safety issues in LIBs for HEVs would be the dendritic lithium ion growth on the anode surface at high charging current, since the conventional carbonous materials approach almost 0 V vs. Li/Li^+ at the end of Li insertion. Recently, various anode materials with improved reversible capacity and stability over commercial graphite have been proposed for Li-ion batteries. Among anode materials, $Li_4Ti_5O_{12}$ has the unique characteristic that the lattice dimension does not change during the reduction to $Li_7Ti_5O_{12}$. A so-called zero-strain lithium insertion material is thus derived [2–4]. It features a flat working voltage of about 1.5 V vs. lithium, which is higher than the reduction potential of common electrolyte solvent. Although $Li_4Ti_5O_{12}$ anode material has many advantages, it cannot meet the need of practical application owing to its poor electronic conductivity [5,6]. To improve the conductivity of $Li_4Ti_5O_{12}$, several effective methods have proposed, including new synthesis method, doping with metal ions or non-metal ions and incorporation of second phase with high electronic conductivity. Studies in $Li_4Ti_5O_{12}$ have been focused on the doped metal ions or conductive surface modification, rather than considering both of them together. Doping with cations and anions in Li, Ti and O was reported [7]. However, up to now, no investigation on the electrochemical characterization of Ru-doped $Li_4Ti_5O_{12}$ as an anode material has been discussed.

In our previous work [8], the electrochemical performance of $Li_4Ti_5O_{12}$ could significantly be improved with a porous structure. Thus, to further improve the electronic conductivity and to reduce the resistance between particles of $Li_4Ti_5O_{12}$, this study aims to individually evaluate the effects of carbon-coated and Ru-doped $Li_4Ti_5O_{12}$, respectively, on the electrochemical performance of $Li_4Ti_5O_{12}$. Finally, combining advantages of both carbon-coated and Ru-doped approach should give better rate performance of $Li_4Ti_5O_{12}$.

2. Experiment

Appropriate amounts of LiCl and 70 wt.% excess $H_2C_2O_4{\cdot}2H_2O$ were thoroughly mixed, and then $TiCl_4$ was rapidly introduced using a dropper. The precursor was mixed and heated at 150 °C for 0.5 h on a hot plate. Finally, it was sintered at 400 °C for 3 h and then calcined at 800 °C for 10 h in air to obtain the $Li_4Ti_5O_{12}$. $Li_4Ru_{0.01}Ti_{4.99}O_{12}$ was synthesized in air by similar method (staring materials: LiCl, $TiCl_4$, $RuCl_3$ and $H_2C_2O_4{\cdot}2H_2O$). For the preparation of carbon-coated $Li_4Ti_5O_{12}$ ($Li_4Ti_5O_{12}$/C), sucrose was selected as the carbon source. Carbon-coated $Li_4Ti_5O_{12}$ was synthesized by dispersing the powder formed after sintering at 400 °C for 3 h

* Corresponding author.
E-mail address: jgd@mx.nthu.edu.tw (J.-G. Duh).

0925-8388/$ – see front matter © 2011 Elsevier B.V. All rights reserved.
doi:10.1016/j.jallcom.2011.04.018

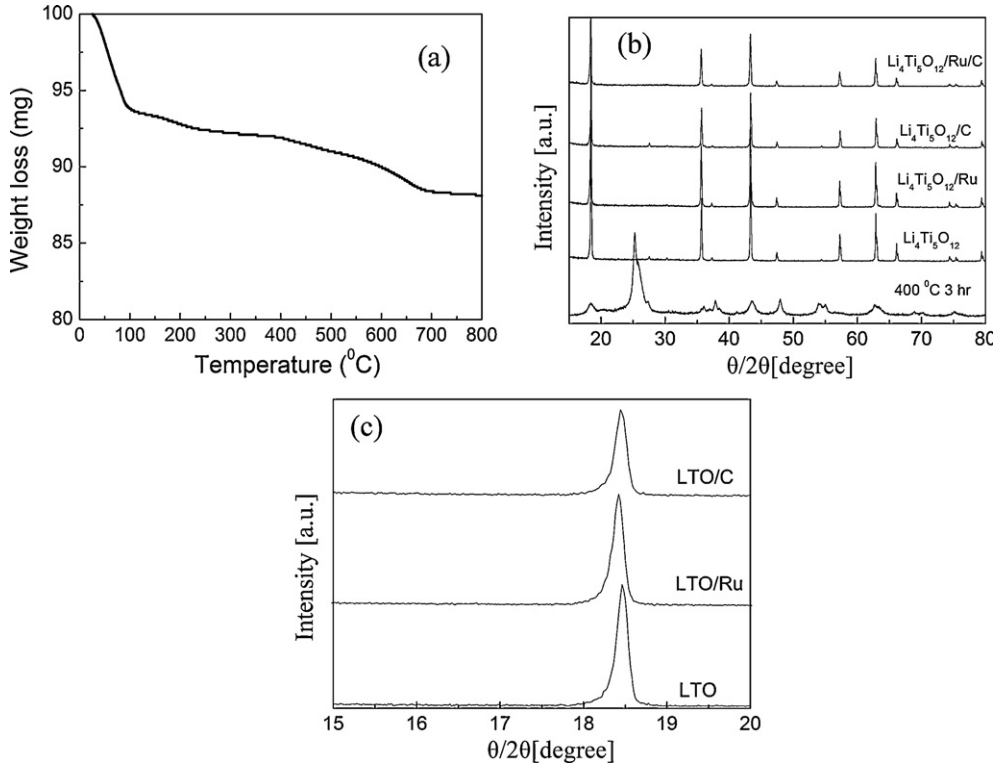

Fig. 1. (a) TGA curves of the precursor of $Li_4Ti_5O_{12}$; (b) the diffraction peaks of the precursor calcined at 400 °C for 3 h, $Li_4Ti_5O_{12}$, $Li_4Ti_5O_{12}$/C, $Li_4Ru_{0.01}Ti_{4.99}O_{12}$ and $Li_4Ru_{0.01}Ti_{4.99}O_{12}$/C calcined at 800 °C for 10 h; (c) enlarged (1 1 1) peaks of $Li_4Ti_5O_{12}$, $Li_4Ti_5O_{12}$/C and $Li_4Ru_{0.01}Ti_{4.99}O_{12}$.

and10 wt.% sucrose in the solution of alcohol. Finally, after removing the solvent, the resulted powder was heated at 800 °C for 10 h in N_2 to synthesize the $Li_4Ti_5O_{12}$/C.

The crystal structure was identified by powder XRD (Rigaku, D/MAX-B, Japan) using Cu Kα radiation at 30 kV and 20 mA. Particle size and morphology of the $Li_4Ti_5O_{12}$ powder were examined with a field emission scanning electron microscope (FE-SEM 7600, JEOL). The element concentration of Li and Ti were confirmed by an inductively coupled plasma-atomic emission spectrometer (ICP-AES, PerkinElmer, Optima 3000DV, U.S.A). The electrode sheets employed for electrochemical examinations were fabricated by mixing active powder with conductive carbon (super P) and binder (PVDF) at a weight ratio of 80:13:7 in N-methyl-2-pyrrolidinone (NMP). The anode sheet was prepared by casting the slurry in Cu foil and drying at 100 °C for 24 h in vacuum. A Li metal disk was used as a cathode and reference in the cell. A 2032 coin cell was fabricated by combining the $Li_4Ti_5O_{12}$ anode and Li metal cathode in a stainless steel button cell containing electrolyte, which was 1 M $LiPF_6$ dissolved in a 1:1 mixture by volume of ethylene carbonate (EC) and dimethyl carbonate (DMC). The cells were assembled in an argon-protected glove box in which water content was kept below 0.1 ppm and all of the cells were cycled within the potential range between 2.5 and 1.0 V at 0.5–10 C rates (1 C = 175 mA).

3. Results and discussion

For the result of TGA analysis as indicated in Fig. 1(a), two mass losses were generally observed. Mass losses below 700 °C are associated with the water release and pyrolysis of the organic compounds. Thus, a synthesized temperature of 800 °C was selected to prepare $Li_4Ti_5O_{12}$ powder. The XRD pattern of the sample obtained at 400 °C for 3 h exhibits the characteristic diffraction lines of anatase TiO_2 and small amounts of $Li_4Ti_5O_{12}$, as shown in Fig. 1(b). Brookite and rutile can intake only small amounts of lithium, while the anatase reacts extensively with stoichiometric up to 0.8–1 Li per Ti [9,10]. The diffraction peaks of the $Li_4Ti_5O_{12}$, $Li_4Ti_5O_{12}$/C, $Li_4Ru_{0.01}Ti_{4.99}O_{12}$ and $Li_4Ru_{0.01}Ti_{4.99}O_{12}$/C are in good agreement with those of the JCPD powder file no. 490207, indicating that the obtained powders have a cubic spinel structure. This implies the added sugar or doped Ru does not affect the spinel structure of $Li_4Ti_5O_{12}$ during heat-treatment. Nevertheless, after detailed examination of the enlarged X-ray diffraction pattern, the (1 1 1) peak of $Li_4Ru_{0.01}Ti_{4.99}O_{12}$ shifted to smaller angles, denoting that the $Li_4Ru_{0.01}Ti_{4.99}O_{12}$ has larger lattice constant than $Li_4Ti_5O_{12}$. The lattice parameter of the $Li_4Ti_5O_{12}$ and $Li_4Ru_{0.01}Ti_{4.99}O_{12}$ obtained according to the Bragg equation was 0.8354 and 0.8372 nm, respectively. This may be attributed to the larger atomic radius Ru^{4+} (0.62 Å) substituting for Ti^{4+} (0.61 Å) [11,12].

The particle size of $Li_4Ti_5O_{12}$, $Li_4Ti_5O_{12}$/C and $Li_4Ru_{0.01}Ti_{4.99}O_{12}$ were analyzed by FE-SEM, as shown in Fig. 2. All the morphologies show homogenous distribution of the particles without serious agglomeration and exhibit a fairly uniform particle size of 400–500 nm. To further understand the distinctions of the $Li_4Ti_5O_{12}$ and $Li_4Ru_{0.01}Ti_{4.99}O_{12}$/C on the electrochemical performance, all the samples were investigated by EIS. Electrochemical impedance spectroscopy (EIS) may be considered as one of the most sensitive tools for studying the changes in the electrode behavior [13]. EIS results of $Li_4Ti_5O_{12}$ and $Li_4Ru_{0.01}Ti_{4.99}O_{12}$/C are shown in Fig. 3. Each plot consisted of one semicircle at higher frequency followed by a linear portion at lower frequency. The low frequency region of the straight line is attributed to the Warburg impedance of long-range lithium ion diffusion. In the equivalent circuit as shown in the inset of Fig. 3(a), R_s indicates the ohmic resistance of electrolyte; R_{ct} is attributed to the charge-transfer resistance at the active material interface; CPE represents the double-layer capacitance and passivation film capacitance. The diffusion coefficient of

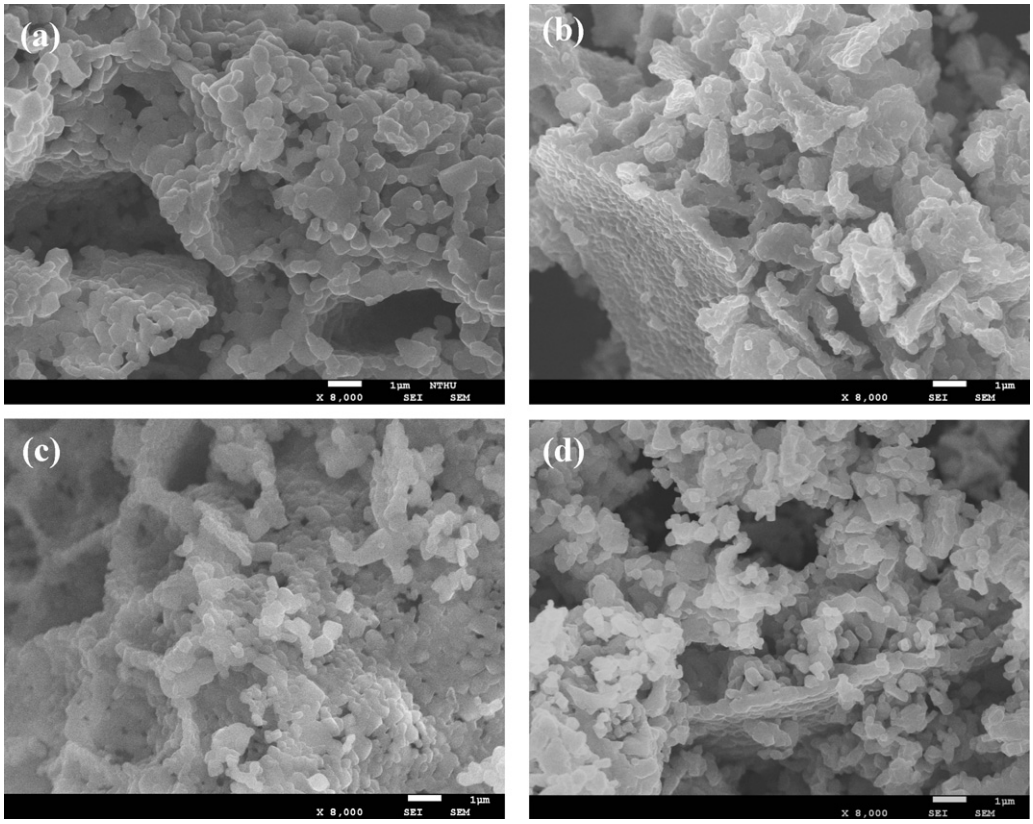

Fig. 2. FE-SEM morphology of (a) $Li_4Ti_5O_{12}$, (b) $Li_4Ti_5O_{12}$/C, (c) $Li_4Ru_{0.01}Ti_{4.99}O_{12}$ and (d) $Li_4Ru_{0.01}Ti_{4.99}O_{12}$/C.

lithium ions diffusing into electrode material were calculated using Eq. (1) [14,15]:

$$D = 0.5\left(\frac{RT}{AF^2\sigma_w C}\right)^2 \quad (1)$$

where σ_w: Warburg impedance coefficient, D: diffusion coefficient, R: the gas constant, T: the absolute temperature, F: Faraday's constant, A: the area of the electrode, and C: molar concentration of Li^+ ions ($C = 1 \times 10^{-3}$ mol cm^{-3}). Table 1 summaries the calculated R_{ct} and diffusion coefficient. It appears that the $Li_4Ru_{0.01}Ti_{4.99}O_{12}$/C exhibited the smallest charge-transfer resistance and largest diffusion coefficient of Li^+ than that of $Li_4Ti_5O_{12}$. After doping Ru and coating carbon, the charge-transfer resistance and diffusion coefficient of $Li_4Ti_5O_{12}$ is effectively improved, which is helpful for the enhancement of rate capability of $Li_4Ti_5O_{12}$ anode material.The electrochemical performance of $Li_4Ti_5O_{12}$, $Li_4Ti_5O_{12}$/C, $Li_4Ru_{0.01}Ti_{4.99}O_{12}$ and $Li_4Ru_{0.01}Ti_{4.99}O_{12}$/C at 0.1 charge/discharge rate is shown in Fig. 4(a). The initial capacity of $Li_4Ti_5O_{12}$, $Li_4Ti_5O_{12}$/C, $Li_4Ru_{0.01}Ti_{4.99}O_{12}$ and $Li_4Ru_{0.01}Ti_{4.99}O_{12}$/C was169, 169, 168 and 168 mAh/g, which is very close to the theoretical capacity 175 mAh g^{-1}.The distinction of electrochemical performance at low charge/discharge rate was rarely detected. $Li_4Ti_5O_{12}$ delivered 167 mAh g^{-1} at 0.5 C charge/discharge rate in Fig. 4(b). However, with the increasing current density, the capacity was133,

Table 1
Impedance parameters of $Li_4Ti_5O_{12}$ and $Li_4Ru_{0.01}Ti_{4.99}O_{12}$/10 wt.%C.

	LTO	LTO/Ru–10 wt.% C
R_{ct} (Ω)	12.9	4.944
σ_w (Ω cm^2/s$^{0.5}$)	7.488	4.5
D (cm^2/s)	3.60×10^{-10}	9.95×10^{-10}

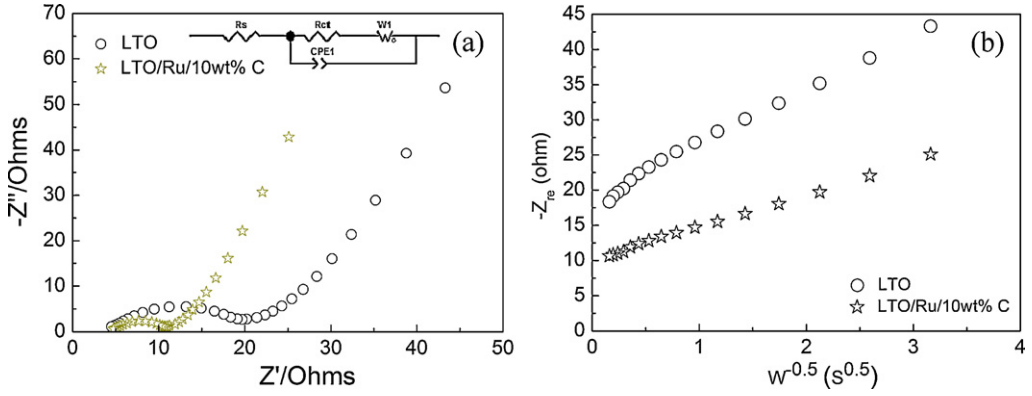

Fig. 3. (a) AC impedance spectra of the $Li_4Ti_5O_{12}$ and $Li_4Ru_{0.01}Ti_{4.99}O_{12}$/C at 1.5 V; (b) the relationship between real impedance and low frequencies for $Li_4Ti_5O_{12}$ and $Li_4Ru_{0.01}Ti_{4.99}O_{12}$/10 wt.%C.

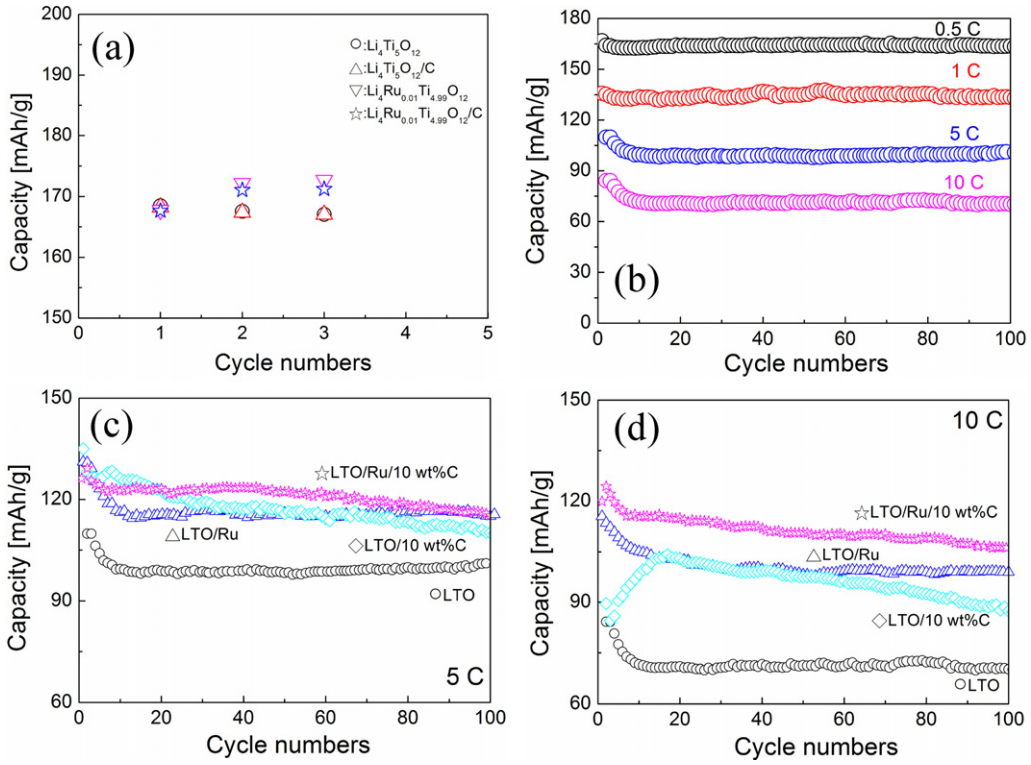

Fig. 4. The electrochemical performance of (a) $Li_4Ti_5O_{12}$, $Li_4Ti_5O_{12}$/10 wt.%C, $Li_4Ru_{0.01}Ti_{4.99}O_{12}$ and $Li_4Ru_{0.01}Ti_{4.99}O_{12}$/10 wt.%C at 0.1 C rate; (b) $Li_4Ti_5O_{12}$ at different charged/discharge rate; (c) $Li_4Ti_5O_{12}$, $Li_4Ti_5O_{12}$/10 wt.%C, $Li_4Ru_{0.01}Ti_{4.99}O_{12}$ and $Li_4Ru_{0.01}Ti_{4.99}O_{12}$/10 wt.%C at 5 C rate; (d) $Li_4Ti_5O_{12}$, $Li_4Ti_5O_{12}$/10 wt.%C, $Li_4Ru_{0.01}Ti_{4.99}O_{12}$ and $Li_4Ru_{0.01}Ti_{4.99}O_{12}$/10 wt.%C at 10 C rate.

100 and 70 mAh/g at 1, 5 and 10 C rate, respectively. The reason for the capacity fading is that the ionic motion within an electrode and/or across an electrode/electrolyte interface is too slow for the charge distribution to reach equilibrium at high current densities [16]. In contrast, the ionic motion of $Li_4Ti_5O_{12}$ at high charge/discharge rate could be improved by carbon-coated $Li_4Ti_5O_{12}$ and doped-Ru $Li_4Ti_5O_{12}$. Fig. 4(c and d) shows the electrochemical properties of $Li_4Ti_5O_{12}$, $Li_4Ti_5O_{12}$/C, $Li_4Ru_{0.01}Ti_{4.99}O_{12}$ and $Li_4Ru_{0.01}Ti_{4.99}O_{12}$/C at 5 and 10 C rates. After coating carbon or doping Ru, the capacity of $Li_4Ti_5O_{12}$/C and $Li_4Ru_{0.01}Ti_{4.99}O_{12}$ exhibited 110, 114 and 88, 100 mAh/g at 5 and 10 C rates, respectively, after 100 cycle numbers, which is higher than pure $Li_4Ti_5O_{12}$. Although the $Li_4Ti_5O_{12}$/C exhibited some capacity loss with charge/discharge cycles, yet $Li_4Ti_5O_{12}$/C still delivered the higher capacity than pure $Li_4Ti_5O_{12}$ at 5 and 10 C rates. The reason for capacity loss of $Li_4Ti_5O_{12}$/C could be ascribedto the following reasons: (1) non-uniform coating on surface of $Li_4Ti_5O_{12}$ and (2) carbon-coating can effectively improve surface electronic conductivity of $Li_4Ti_5O_{12}$, but cannot improve the intrinsic electronic conductivity of $Li_4Ti_5O_{12}$. However, it is evident that the Ru-doped $Li_4Ti_5O_{12}$ exhibits better cyclic retention than $Li_4Ti_5O_{12}$/C. The $Li_4Ru_{0.01}Ti_{4.99}O_{12}$/C shows the highest capacity (110 mAh/g) and the best cycling retention at 10 C rate after 100 cycle numbers among samples of $Li_4Ti_5O_{12}$, $Li_4Ti_5O_{12}$/C and $Li_4Ru_{0.01}Ti_{4.99}O_{12}$. As a result, combining the Ru-doped and carbon-coated techniques to fabricate $Li_4Ru_{0.01}Ti_{4.99}O_{12}$/C effectively enhance the diffusion rate of Li^+ and significantly reduce surface electronic resistance of $Li_4Ti_5O_{12}$.

4. Conclusion

$Li_4Ti_5O_{12}$, $Li_4Ti_5O_{12}$/C and $Li_4Ru_{0.01}Ti_{4.99}O_{12}$ and $Li_4Ru_{0.01}Ti_{4.99}O_{12}$/C were successfully synthesized by a modified solid-state method. The XRD pattern showed that both the carbon-coating and Ru-doping does not alter the spinel structure of $Li_4Ti_5O_{12}$. The $Li_4Ti_5O_{12}$, $Li_4Ti_5O_{12}$/C, $Li_4Ru_{0.01}Ti_{4.99}O_{12}$ and $Li_4Ru_{0.01}Ti_{4.99}O_{12}$/C deliver 70, 88, 100 and 110 mAh/g at 10 C rate after 100 cycle numbers. From the EIS and electrochemical performance results, the $Li_4Ru_{0.01}Ti_{4.99}O_{12}$/C revealed the lowest charge-transfer resistance and the better rate capability at high charge/discharge *C* rate, indicating that the carbon-coating and Ru-doping are effective methods to improve the electrochemical performance of $Li_4Ti_5O_{12}$.

Acknowledgment

This study was financially supported by National Science Council of Taiwan, under project No. NSC 96-2221-E-007-093-MY3 and from the Ministry of Economics under the project No. 98-EC-17-A-08-S1-003.

References

[1] K. Ariyoshi, Y. Makimura, T. Ohzuku, Lithium Insertion Materials having Spinel-Framework Structure for Advanced Batteries, Wiley-VCH, Weinheim, 2009.
[2] M. Venkateswarlu, C.H. Chen, J.S. Do, C.W. Lin, T.C. Chou, B. Hwang, J. Power Sources 146 (2005) 204.
[3] J.L. Allen, T.R. Jow, J. Wolfenstine, J. Power Sources 159 (2006) 1340.
[4] J.J. Huang, Z.Y. Jiang, Electrochim. Acta 53 (2008) 7756.
[5] Z. Lin, X. Hu, Y. Huai, L. Liu, Z. Deng, J. Suo, Solid State Ionics 181 (2010) 412.
[6] P.P. Prosini, R. Mancini, L. Petrucci, V. Contini, P. Villano, Solid State Ionics 144 (2001) 185.
[7] T.F. Yi, L.J. Jiang, J. Shu, C.B. Yue, R.S. Zhu, H.B. Qiao, J. Phys. Solids 71 (2010) 1236.
[8] C.Y. Lin, J.G. Duh, J. Alloys Compd. 509 (2011) 3682.
[9] T. Yuan, R. Cai, P. Gu, Z. Shao, J. Power Sources 195 (2010) 2883.
[10] M.W. Raja, S. Mahanty, M. Kundu, R.N. Basu, J. Alloys Compd. 468 (2009) 258.
[11] X. Li, M. Qu, Z. Yu, J. Alloys Compd. 487 (2009) L12.
[12] B. Tian, H. Xiang, L. Zhang, Z. Li, H. Wang, Electrochim. Acta 55 (2010) 5453.
[13] A.Y. Shenouda, H.K. Li, J. Power Sources 185 (2008) 1386.
[14] X. Li, M. Qu, Z. Yu, Solid State Ionics 181 (2010) 635.
[15] X. Li, M. Qu, Y. Huai, Z. Yu, Electrochim. Acta 55 (2010) 2978.
[16] J. Goodenough, Y. Kim, Chem. Mater. 22 (2010) 587.